Finally, we return to the behavior of the resistivity during annealing. This is shown in Fig. 8 for the case of $I_0=10^{-4}$ and $B=0.25$ ev. Since the relative magnitudes of ρ_I and ρ_c are not usually available, several values of $\beta=(\rho_c-\rho_I)/\rho_v$ are assumed. It is clear that resolution of recovery into two stages is still present. A small rise in resistivity in the intermediate temperature range may or may not be measurable depending on the pertinent values of I_0, B, and β. Presumably, the simplest manner to attempt to observe such a rise would be to use a metal where $I_0\approx 10^{-3}$ or somewhat greater.

The results presented in the previous sections are basically more general than it may first appear. A particular model has been used only to demonstrate the various features of defect recovery. Obviously, interstitial atoms may migrate and be bound in a manner formally equivalent to vacancies.

ACKNOWLEDGMENTS

It is a pleasure to acknowledge the aid of A. G. Presson and J. E. Mericle in carrying through the computer calculations.

PHYSICAL REVIEW VOLUME 122, NUMBER 4 MAY 15, 1961

Polarization of Co^{57} in Fe Metal*

J. G. DASH,† R. D. TAYLOR, D. E. NAGLE, P. P. CRAIG, AND W. M. VISSCHER
Los Alamos Scientific Laboratory, University of California, Los Alamos, New Mexico
(Received December 16, 1960)

A study has been made of the effect of low temperatures on the resonant emission and absorption of 14.4-kev Mössbauer radiation from Fe^{57} in Fe metal. Analysis of intensity changes in the hyperfine spectrum is made in terms of the Zeeman level splittings of the ground states of Fe^{57} absorbing nuclei and of the ground states of Co^{57} parent nuclei. The theory for the temperature dependence is developed in terms of the properties of the Co^{57} decay and of the subsequent gamma transitions. Experiments were carried out with a source of Co^{57} nuclei in Fe metal at temperatures between 4.5° and 0.85°K. The experimental results, analyzed in terms of the theory, yield a value of the hyperfine magnetic field at the Co^{57} nuclei. Comparison of the result with other pertinent experimental values indicates that depolarization of the nuclei by the K-capture decay of Co^{57} is not evident in the present material.

I. INTRODUCTION

THE 14.4-kev gamma rays of Fe^{57} nuclei are known to have, in suitable crystals, a high proportion f of recoil-free, or "Mössbauer" radiation.[1-4] Interest in the Fe^{57} system is enhanced by the relatively narrow linewidths characteristic of the excited state (lifetime 10^{-7} sec) and the clearly resolvable hyperfine components of the Mössbauer pattern. Experiments with Fe crystal sources and absorbers are facilitated by the large value of f even at room temperature as a consequence of the high Debye characteristic temperature ($\Theta\simeq 420$°K) and the low nuclear recoil temperature ($T_R\simeq 40$°K). A source of Co^{57} nuclei dissolved in a Fe lattice at room temperature has $f\simeq 0.7$[1]; cooling the source to 0°K increases f to 0.92. This limit is achieved to within 0.1% by 20°K, and similar "saturation" obtains for the fraction f' of recoil-free absorption by an absorber of Fe^{57} in Fe metal. Further cooling will result in a negligible increase of f and f'; cryogenic studies of the system might appear unprofitable.

At sufficiently low temperatures, however, a redistribution of the populations of the Zeeman sublevels takes place, and the nuclei become polarized.[5] This polarization can be quantitively studied through the effect upon the hyperfine Mössbauer spectrum. While nuclear polarization in ferromagnets has been observed before,[6] the present technique offers certain advantages. In this type of experiment the magnitude and sign of the magnetic field at the Co nucleus may be determined. The effects of the nuclear polarization are the concern of this paper.

II. Fe^{57} IN Fe METAL

The ground state of Co^{57}, with a half-life of 270 days, decays by K-electron capture and neutrino emission to the second excited state of Fe^{57}. The decay is probably an allowed transition, since its value of $\log ft=6$ lies

* Work performed under the auspices of the U. S. Atomic Energy Commission.
† Present address, University of Washington, Seattle, Washington.
[1] R. V. Pound and G. A. Rebka, Jr., Phys. Rev. Letters **3**, 554 (1959).
[2] J. P. Schiffer and W. Marshall, Phys. Rev. Letters **3**, 556 (1959).
[3] G. de Pasquali, H. Frauenfelder, S. Margulies, and R. N. Peacock, Phys. Rev. Letters **4**, 71 (1960).
[4] S. S. Hanna, J. Heberle, C. Littlejohn, G. J. Perlow, R. S. Preston, and and D. H. Vincent, Phys. Rev. Letters **4**, 177 (1960).
[5] J. G. Dash, R. D. Taylor, P. P. Craig, D. E. Nagle, D. R. F. Cochran, and W. E. Keller, Phys. Rev. Letters **5**, 152 (1960).
[6] M. J. Steenland and H. A. Tolhoek, *Progress in Low-Temperature Physics*, edited by C. J. Gorter (Interscience Publishers, Inc., New York, 1957), Vol. II, Chap. X, p. 292.

within the limits of logft for known allowed transitions,[7] and this agrees with accepted spin assignments and considerations based on the shell model. The nuclear spin I_3 of Co^{57} is 7/2, and its magnetic moment μ_3 is 4.65 nm.[8] The second excited state of Fe^{57} has spin I_2 of 5/2 and a mean lifetime of about 9×10^{-9} sec.[9] This state decays, by emission of a 123-kev gamma ray, to the first excited state of Fe^{57}. A minor fraction (9%) of the decays involve a transition from the second excited state directly to the ground state, with the emission of a 137-kev gamma ray.[10] The multipolarity of the 123-kev radiation is 96% $M1$, 4% $E2$.[9,11] The first excited state has spin $I_1=3/2$, and moment μ_1 of 0.153 nm.[4] This state has a half-life of 1.1×10^{-7} sec, and decays by pure $M1$ emission of a 14.4-kev gamma ray, to the ground state of Fe^{57}. The spin of the ground state, I_0, is 1/2, and it has a moment μ_0 of 0.0903 nm.[12] Experiments on the Mössbauer effect have been used to obtain a detailed description of the first excited and ground states of Fe^{57} in Fe metal.[4] Results of this study, together with the properties of the higher states, are shown in Fig. 1. We also show the normal order of sublevels of Co^{57}, deduced from preliminary results[5] of the study reported here.

The hyperfine magnetic field H acting on equivalent nuclei in a ferromagnetic crystal has a single direction in space over the region of a ferromagnetic domain. Coupling between the nuclear magnetic moments and the hyperfine field removes the degeneracy of nuclear spin orientation and produces a set of equally spaced spin sublevels of energies $\Delta E_{\rm hfs}=mg\mu_n H$, $-I\leq m\leq I$, where m is the magnetic quantum number, g is the nuclear gyromagnetic ratio, and μ_n is the nuclear magneton. In cubic Fe metal, all nuclei occupy equivalent lattice positions; hence, there is a single preferred direction in space and a single set of energy sublevels for the Fe nuclei in each ferromagnetic domain. An unmagnetized sample has its domains oriented in several directions, such that there is no net spatial polarization of the entire sample, but all of the nuclei (excepting those in the neighborhood of imperfections and impurities, and possibly those near domain walls) have the same hyperfine level splittings. The splittings of the first excited and ground states of Fe^{57} are greater than the linewidth of the 14.4-kev resonance radiation. Gamma-ray transitions between the 14.4-kev sublevels of magnetic quantum number m_j to the ground-state

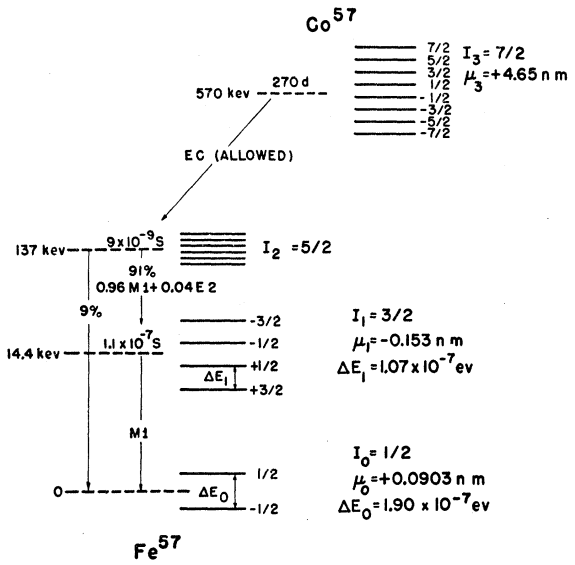

FIG. 1. Energy level diagram of Co^{57} and daughter nuclei.

sublevels m_k ($m_k=m_j, m_j\pm1$), therefore result in a gamma-ray spectrum of six hyperfine components. The relative intensity of the transition ($m_j\rightarrow m_k$) is proportional to the probability w_{jk} specified by the rules governing magnetic dipole radiation. Figure 2 is a schematic diagram of the radiation, similar to a diagram given by Hanna *et al.*[4] The radiation widths are suppressed, and relative intensities are appropriate to the case of unpolarized radiation from a source having no net magnetization.[12a] Positions of the line centers are given in terms of Doppler velocity shifts (positive velocity taken as increasing separation between source and detector) equivalent to shifts from the energy difference between degenerate excited and ground states. The m values of the upper and lower state sublevels are shown at the top and bottom of each line.

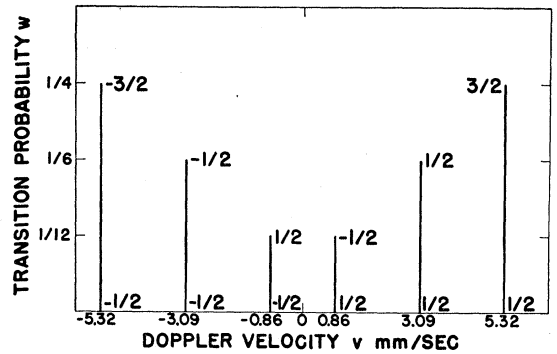

FIG. 2. Schematic diagram of the recoil-free 14.4-kev radiation from Fe^{57} in Fe metal. Individual linewidths are not shown. Relative transition probabilities are appropriate to the case of domains oriented at random. Energy displacements are in terms of Doppler velocity, positive velocity being taken as increasing separation between source and observer. Magnetic sublevel quantum numbers for the first excited and ground states are shown at top and bottom, respectively, of each line.

[7] B. L. Robinson and R. W. Fink, Revs. Modern Phys. **32**, 117 (1960).
[8] J. M. Baker, B. Bleaney, P. M. Llewellyn, and P. F. D. Shaw, Proc. Phys. Soc. (London) **A69**, 353 (1956).
[9] G. F. Pieper and N. P. Heydenburg, Phys. Rev. **107**, 1300 (1957).
[10] D. E. Alburger and M. A. Grace, Proc. Phys. Soc. (London) **A67**, 280 (1954).
[11] G. R. Bishop, M. A. Grace, C. E. Johnson, A. C. Knipper, H. R. Lemmer, J. Perez y Torba, and R. G. Scurlock, Phil. Mag. **46**, 951 (1955).
[12] G. W. Ludwig and H. H. Woodbury, Phys. Rev. **117**, 1286 (1960).

[12a] See "note added in proof."

An absorber of Fe^{57} in Fe metal has a similar hyperfine pattern of resonant cross sections. If Fig. 2 is translated over an identical pattern, the overlaps at velocity differences $v=v(\text{source})-v(\text{absorber})$ represent the absorption dips obtained when a source is moved relative to an absorber, resulting in a Mössbauer-type intensity pattern. As a result of chemical or temperature differences between source and absorber, the emission and absorption spectra are shifted relative to each other by a small Doppler velocity δv.[13,14] This shift is not essential to the present study, and the relative velocities v will be understood to represent the displacements from δv.

III. THEORY

Polarization and Depolarization

The intensity of the emission line $(m_j \rightarrow m_k)$ is proportional to the transition probability w_{jk} and to the population p_j of the sublevel at which the transition originates. We define W_{jk} as the normalized relative intensity

$$W_{jk}=p_j w_{jk}/\sum_{jk} p_j w_{jk}. \quad (1)$$

In thermal equilibrium the populations p_j are proportional to the Boltzmann factors of the nuclear sublevels. The nuclear spins of the first excited state of Fe^{57}, however, are not in thermal equilibrium. Gossard and Portis[15] have measured a spin relaxation time of 10^{-4} sec for Co^{59} nuclei in Co metal, and one may expect the relaxation time to increase as T^{-1} at lower temperatures.[16] The relaxation mechanisms for Co and Fe nuclei in Fe metal should be quite similar to those in the Co metal, and we may therefore treat the spin populations of the 14.4-kev state of Fe^{57} as unchanged during the 10^{-7} sec state lifetime. Since the lifetime of the second excited state is even shorter than 10^{-7} sec, the p_j of a source of 14.4-kev radiation are functions of the populations of sublevels in the 270-day Co^{57} parent. The equilibrium population p_l of the Co^{57} sublevel, in the case of pure magnetic hfs, is given by the Boltzmann factor:

$$p_l=C\exp(m_l\xi T^{-1}), \quad \text{where} \quad \xi=g\mu_n H k^{-1}; \quad (2)$$

m_l is the magnetic quantum member of the sublevel, T is the temperature, $g\mu_n$ is the moment of the Co^{57} nucleus, H is the hyperfine magnetic field at the nucleus, k is Boltzmann's constant, and C is a constant. A Co^{57} nucleus in the m_l sublevel decays to the m_j sublevel of the 14.4-kev state of Fe^{57} with a probability Q_{lj}. The matrix Q is the product of Clebsch-Gordan matrices for the two transitions preceding the arrival at the 14.4-kev state, and is presented in the Appendix. We can therefore obtain the p_j of the 14.4-kev state by summing contributions from the parent sublevels:

$$p_j=\text{const}\sum_l p_l Q_{lj}. \quad (3)$$

Substituting Eqs. (2) and (3) in Eq. (1), we obtain the relative intensity of an emission line $(m_j \rightarrow m_k)$ of a source,

$$W_{jk}=w_{jk}\sum_l e^{m_l\xi/T}Q_{lj}/(\sum_{jk} w_{jk}\sum_l e^{m_l\xi/T}Q_{lj}). \quad (4)$$

We have assumed that spin lattice relaxation causes negligible depolarization of the spins during the K capture and subsequent gamma emissions. A second possible mechanism for depolarization is due to perturbations by extranuclear fields resulting from K capture. A study of the angular distribution of the 123-kev radiation from partially aligned Co^{57} nuclei in a Tutton salt[11] indicated considerable depolarization of the second excited state, presumably as a result of the K-capture process. Depolarization to the extent observed in the Tutton salt would cause a marked decrease in the population asymmetries. We believe at the outset, however, that the large electron mobilities in the Fe metal provide a rapid extinction of the perturbing fields, making depolarization much smaller than in the salt.

Transmitted Intensities

We consider a resonance emission spectrum composed of several lines of Lorentzian shape, each line having the width Γ. The relative intensity of a line centered at energy E_{jk} is W_{jk}. When the source of radiation is moving away from the observer at speed v, the intensity distribution of the $(m_j \rightarrow m_k)$ line is given by

$$g_{jk}(v)=\frac{I\Gamma/2\pi}{(E-E_{jk}+E_{jk}v/c)^2+\Gamma^2/4}, \quad (5)$$

where I is the total intensity,

$$I=\sum_{jk} W_{jk}\int_0^\infty g_{jk}(v)dE. \quad (6)$$

The hyperfine emission spectrum of a source can be analyzed by filtering the radiation through an absorber containing ground-state nuclei: in the present case, Fe^{57}. Absorbing nuclei are excited from ground-state sublevels to sublevels of the first excited state, and the transitions $(m_{k'} \rightarrow m_{j'})$ have relative "intensities" $W_{k'j'}$, where the primed symbols represent the absorber. The hyperfine resonant absorption cross section is composed of lines of cross section $W_{k'j'}\sigma_{k'j'}$, where

$$\sigma_{k'j'}=\frac{\sigma\Gamma^2/4}{(E-E_{k'j'})^2+\Gamma^2/4}, \quad (7)$$

[13] R. V. Pound and G. A. Rebka, Jr., Phys. Rev. Letters 4, 274 (1960).
[14] B. D. Josephson, Phys. Rev. Letters 4, 341 (1960).
[15] A. C. Gossard and A. M. Portis, Phys. Rev. Letters 3, 164 (1959).
[16] G. E. Pake, in *Solid State Physics*, edited by F. Seitz and D. Turnbull (Academic Press, Inc., New York, 1956), Vol. 2.

and σ is the total resonant absorption cross section. If such an absorber is placed between a source of radiation as is represented by Eq. (5), the intensity transmitted at relative Doppler speed v is

$$I_t(v)=\sum_{jk} W_{jk}\int_0^\infty g_{jk}(v) \times\exp[-naf'\sum_{k'j'} W_{k'j'}\sigma_{k'j'}]dE, \quad (8)$$

where n is the total number of atoms/cm^2 in the absorber, a is the abundance of the isotope which absorbs resonantly, and f' is the fraction of recoil-free resonant absorptions.[17]

The overlap integral of Eq. (8) is implicitly limited to the case of unpolarized spectra obtained with unmagnetized sources and absorbers. In the event of a net magnetization it is necessary to take account of the relative orientations of the magnetic fields acting on the source and absorber nuclei. We will, however, limit this treatment to the case of unpolarized radiation, such as is represented in Fig. 2. The integral in Eq. (8) can be solved in closed form for two special cases: either perfect overlap of emission and absorption lines, or for no overlap. The latter case is equivalent to no resonant absorption, the transmitted intensity then being given by Eq. (6). In the case of perfect overlap, when an emission line energy E_{jk} is Doppler shifted so that $E_{jk}(1-v/c)=E_{k'j'}$, the transmitted jk line intensity $I_t(jk)$ can be written

$$I_t(jk)=\frac{I}{\pi}W_{jk}\int_{-\infty}^{\infty}\frac{dy}{1+y^2}\exp\left[\frac{-W_{k'j'}x}{1+y^2}\right], \quad (9)$$

where $y=2(E-E_{k'j'})/\Gamma$, and $x=naf'\sigma$. The solution of Eq. (9) is

$$I_t(jk)=IW_{jk}J_0(iW_{k'j'}x/2)\exp(-W_{k'j'}x/2), \quad (10)$$

where J_0 is the Bessel function of zeroth order. We shall assume that the 14.4-kev spectrum given in Fig. 2 represents both the emission spectrum of the source and the absorption pattern of the absorber. The overlap, or Mössbauer, pattern of such a source-absorber combination has several discrete Doppler speeds V at which the transmitted intensity due to all emission lines can be expressed in terms of the two special cases given above. Although the Lorentzian form of the lines vanishes only at infinity, a separation of 5Γ between source and absorption line energies is sufficient to reduce the resonant absorption to less than 1% of that at perfect overlap. We shall adopt this separation as a practical criterion for the absence of overlap. There are then four speeds V at which we can evaluate the transmitted intensity with good accuracy: These speeds are 2.23, 6.18, 8.41, and 10.46 mm/sec. The overlap and no-overlap contributions can be distinguished by a function Δ_V having the properties:

$$\begin{aligned}&\Delta_V=1, \quad \text{when} \quad E_{jk}(1-V/c)=E_{k'j'},\\ &\Delta_V=0, \quad \text{when} \quad |E_{jk}(1-V/c)-E_{k'j'}|>5\Gamma.\end{aligned} \quad (11)$$

The intensity transmitted at one of these discrete speeds can then be obtained by summing the contributions of overlapping and nonoverlapping lines:

$$I_t(V)=I\sum_{jkk'j'} W_{jk} \times\{1-\Delta_V[1-J_0(iW_{k'j'}x/2)\exp(-W_{k'j'}x/2)]\}. \quad (12)$$

The hyperfine radiation is, in practice, associated with a broad background of nonresonant gamma rays, and the absorber has a certain amount of nonresonant absorption. The nonresonant background to the Mössbauer pattern can be formally eliminated by comparing transmitted intensities at speed V with the intensity transmitted at high speed. The results of our experiment are expressed as a ratio,

$$R(V)\equiv[I_\infty-I_t(V)]/[I_\infty-I_t(-V)], \quad (13)$$

where I_∞ is the intensity transmitted at speeds high enough so that no lines overlap, and $I_t(V)$ and $I_t(-V)$ are the intensities transmitted at $+V$ and $-V$, respectively. The explicit dependence of $R(V)$ on the relative intensities of source and absorber lines is obtained by substituting Eq. (12) in Eq. (13):

$$R(V)=\sum_{jkk'j'}\Delta_V W_{jk}K_{k'j'}(x)/\sum_{jkk'j'}\Delta_{-V}W_{jk}K_{k'j'}(x), \quad (14)$$

where

$$K_{k'j'}(x)=1-J_0(iW_{k'j'}x/2)\exp(-W_{k'j'}x/2).$$

We wish to obtain the explicit dependence of $R(V)$ on the temperature of the source or of the absorber. Each case will be treated separately in the following sections.

Cold Source

We assume the absorber to be sufficiently warm so that we can neglect differences between sublevel populations in the absorber: $W_{k'j'}=w_{k'j'}/\sum_{k'j'}w_{k'j'}$. The temperature dependence of $R(V)$ then arises from the differences in Boltzmann factors of the Co^{57} sublevels and their influence on relative line intensities, Eq. (4). Before making the indicated substitution for W_{jk} in Eq. (14), we note a symmetry property of the hyperfine spectrum, Fig. 2: If emission line (j,k) overlaps absorption line (k',j') at relative velocity V, then $(-j,-k)$ overlaps $(-k',-j')$ at velocity $-V$. Furthermore, the transition probabilities of symmetric lines are equal:

$$w_{jk}=w_{-j-k}, \quad \text{and} \quad w_{k'j'}=w_{-k'-j'}.$$

Making use of these relations, substituting Eq. (4) in

[17] P. P. Craig, J. G. Dash, A. D. McGuire, D. Nagle, and R. D. Reiswig, Phys. Rev. Letters 3, 221 (1959).

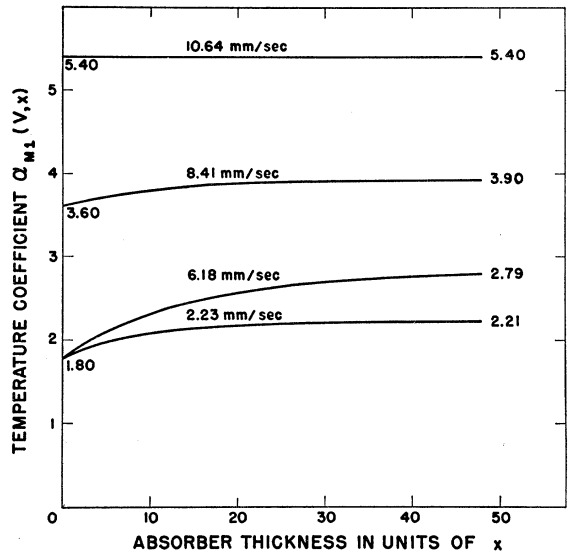

FIG. 3. Calculated temperature coefficients of several relative absorption-emission velocities as a function of the thickness parameter x.

Eq. (14) yields

$$R(V)=\frac{\sum_{jkk'j'}\Delta_V K_{k'j'}(x)w_{jk}\sum_l e^{m_l\xi/T}Q_{lj}}{\sum_{jkk'j'}\Delta_V K_{k'j'}(x)w_{jk}\sum_l e^{m_l\xi/T}Q_{l-j}}=\frac{\sum_{jkk'j'}\Delta_V K_{k'j'}(x)w_{jk}\sum_l e^{m_l\xi/T}Q_{lj}}{\sum_{jkk'j'}\Delta_V K_{k'j'}(x)w_{jk}\sum_l e^{-m_l\xi/T}Q_{lj}}, \quad (15)$$

since $Q_{lj}=Q_{-l-j}$. Equation (15) takes a simple form at relatively high temperatures, when $\xi/T\ll 1$. Expanding the Boltzmann factors to first order in ξ/T, we obtain the high-temperature approximation,

$$R(V)=1+\alpha(V,x)\xi T^{-1}, \quad (16)$$

where

$$\alpha(V,x)=\frac{2\sum_{jkk'j'}\Delta_V K_{k'j'}(x)w_{jk}\sum_l m_l Q_{lj}}{\sum_{jkk'j'}\Delta_V K_{k'j'}(x)w_{jk}\sum_l Q_{lj}}. \quad (17)$$

The decay from the first excited state to the ground state of Fe^{57} is pure $M1$. There is, however, a mixture of $M1$ and $E2$ gamma rays in the decay from the second to first excited states. If we assume that the mixture is incoherent, as for the unpolarized spectra from unmagnetized sources, the temperature coefficient will have a similar mixture:

$$R(V)=1+[0.96\alpha_{M1}(V,t)+0.04\alpha_{E2}(V,t)]\xi T^{-1}, \quad (18)$$

where α_{M1} and α_{E2} are the coefficients corresponding to Eq. (17) with the proper matrix elements Q_{lj} for $M1$ and $E2$ radiation, respectively.

The temperature coefficient $\alpha_{M1}(V,x)$ for each speed V is shown as a function of the thickness parameter in Fig. 3. Coefficients $\alpha_{E2}(V,x)$ are approximately one-half to one-third of the corresponding factor for the $M1$ radiation: The coefficient representing all of the transitions can therefore be estimated as 98% of the $\alpha_{M1}(V,x)$.

Cold Absorber

The temperature dependence of $R(V)$ for a warm source and a cold absorber is related to the splitting of the ground-state levels of Fe^{57} in the absorber, and is independent of the hfs of the ground state of Co^{57}. Therefore, this case does not depend on the matrix elements Q_{lj}, and the analysis is accordingly simpler. Also, no depolarization or coherence effects are present as considered above. Since we have not investigated this arrangement experimentally, we will only approximate the temperature dependence. The approximation considered is that of a thin absorber, $xW_{k'j'}/2\ll 1$. Expanding $K_{k'j'}(x)$ to first order in x, and expressing the relative strength $W_{k'j'}$ of an absorption line in terms of the population $p_{k'}$ of the ground-state sublevel,

$$K_{k'j'}(x)\simeq xW_{k'j'}/2=xp_{k'}w_{k'j'}/(2\sum_{k'j'}p_{k'}w_{k'j'}). \quad (19)$$

The most convenient overlap speeds for exploring the dependence of $R(V)$ on absorber temperature are those at $V=6.18$, 8.41, and 10.46 mm/sec. At these moderately strong absorption dips, all overlaps at $+V$ are due to absorption lines arising from the $+1/2$ ground-state sublevel, and all at $-V$ originate from the $-1/2$ sublevel. Equation (14) reduces, for these cases, to the particularly simple form:

$$R(V)=p_{\frac{1}{2}}/p_{-\frac{1}{2}}=\exp(\xi_0 T^{-1}), \quad (20)$$

where $\xi_0 k$ is the energy splitting of the ground-state sublevels.

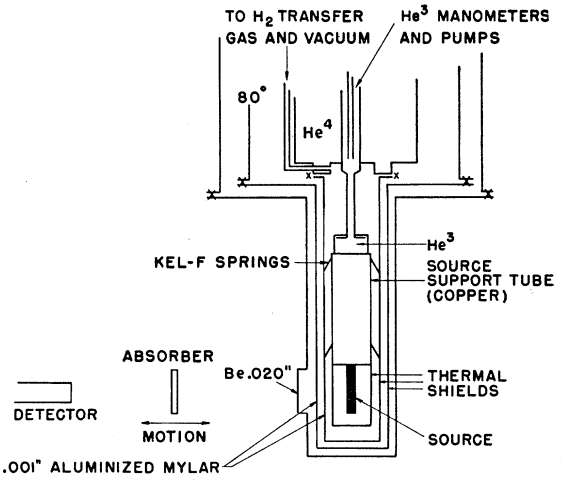

FIG. 4. Schematic diagram of the experimental arrangement.

IV. EXPERIMENTAL APPARATUS

A schematic diagram of the experimental arrangement is shown in Fig. 4. The cryostat has a somewhat unconventional design in that no liquid extends down to the height of the sample. The source is thermally protected by three concentric copper shields, the tops of which are maintained at liquid N_2, liquid He^4, and liquid He^3 temperatures. These features permit the 14-kev radiation to leave the cryostat with an attenuation due only to thin windows in the shields; namely, 0.001-in. Al at He^3 temperatures, 0.001-in. aluminized Mylar plastic at 1.4°K and 80°K, and 0.020-in. Be at room temperature. The source was connected directly to the He^3 reservoir via a heavy copper tube held rigidly in place within the He^4 shield by means of compressed leaf springs made of Kel-F plastic. The flange at the top of the He^4 shield was sealed to the He^4 reservoir by means of a Sn-In O-ring.

The desired temperature was reached and maintained by controlling the pumping rate on the He^3 bath. Temperatures were determined from the observed He^3 bath vapor pressures and a carbon resistance thermometer attached to the source holder.

The 10-millicurie source was prepared in the manner described by Pound and Rebka.[1] Co^{57} was plated from a $Co^{57}Cl_2$ solution on a 0.007-in. thick of Armco iron which was then annealed in vacuum for approximately one hour at 900°C to cause diffusion of the Co^{57} into the Fe lattice. The thin sheet was soft soldered to a copper holder for rigidity and good thermal contact.

Absorbing foils of Fe^{57} metal were prepared either by plating the enriched isotope on 0.1-mil Ni foil or by rolling sheets of the enriched Fe metal. The rolled foils were made by a technique used by Karasek of the Argonne National Laboratory.[18] A button of 78% Fe^{57}, 22% Fe^{56}, was rolled to approximately 1-mil thickness in successive stages during which the sheets were annealed several times. The 1-mil sheet was further reduced by "pack rolling" between ferrotype plates, to approximately 0.1 mil. The foil was clamped between thin sheets of Mylar plastic by a soft iron frame holder.

The detector consisted of a 1-mm thick NaI(Tl) crystal sealed to an RCA 6342 photomultiplier tube. Scintillation pulses corresponding to energies in the neighborhood of 14 kev were counted by means of a Franklin Model 358 amplifier and single-channel analyzer, a modified Berkeley Model 7161–3 counter and a digital recorder.

The absorber foils were mounted on a sliding carriage whose mean position was 20 cm in front of the scintillator crystal. A cable system drove the carriage at fixed linear speeds over a 6-cm horizontal path. This drive consisted of a 1/25-hp synchronous motor, worm gear speed reducers, and a 40-speed lathe gear box. Microswitches at each end of the carriage path reversed the motor, and after an initial absorber travel of about 1 cm, the microswitches automatically reset and started the counter. The timing interval on the counter could be preset to four significant figures, so that counting could be made over almost the same absorber path at any given speed. This procedure averaged the measured intensities over nearly the same path length for positive and negative velocities, and was found to be necessary because of a 1% difference in counting rates between the extremes of absorber travel. The gear box and three interchangeable worm gear reducers allowed a choice of 120 Doppler speeds, ranging from 0.0143 to 14.94 mm/sec at a motor speed of 1800 rpm. Intervals between the speed settings were adequate to explore the shape of the central absorption peak, but were in some cases too coarse to examine the details of other lines. We therefore used a vernier control on the speed by running the synchronous motor at power frequencies between 50 and 70 cps. The variable frequency power was generated by two audio oscillators and a power amplifier; the two oscillators were used alternately for positive and negative absorber velocities. This scheme made compensation possible for the small temperature and chemical shifts of the resonance patterns by setting the oscillators to different frequencies. The oscillator frequencies were measured and found to be stable to better than 0.1%. A 100-kc/sec crystal driven chronograph and optical gating system showed the absorber speeds to be uniform and stable to better than 0.03% over the whole length of travel when the motor was driven by the 60-cps power line. When two frequencies were used to drive the motor, the path length for the velocity corresponding to the lower drive frequency was slightly shorter because the preset timer on the counter was not alternated: The effect on the data is discussed in the next section. Unwanted relative motion of the source with respect to the absorber due to lateral vibration of the source within the cryostat was reduced by means of the Kel-F spacers. With this internal bracing, the assembly approached the rigidity of the outer casing of the cryostat; this in turn was fixed to the platform which supported the absorber carriage. Rigidity and good thermal isolation of the colder regions of the cryostat are somewhat incompatible; it was necessary to reach a compromise between the two extremes.

Experimental Results

The absorbers used were a plated foil of 2 mg/cm² Fe^{57} and a rolled foil of 1.73 mg/cm² Fe^{57}. Although both foils had comparable resonance absorptions, the rolled foil was better in two respects; it had a narrower line and a smaller resonance pattern shift when both source and absorber were at room temperature. This shift was approximately 1.2×10^{-2} mm/sec, equivalent to a fractional resonant frequency difference between source and absorber of $\Delta\nu/\nu=4\times10^{-15}$, and could be accounted for by a difference between the characteristic Debye

[18] S. S. Hanna (private communication).

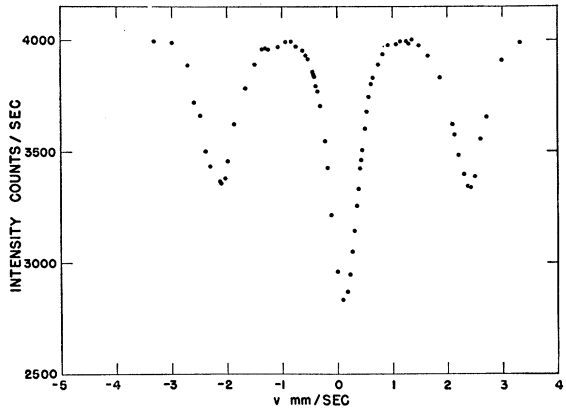

FIG. 5. Experimental overlap pattern of Fe^{57} in Fe metal, for Doppler speeds between 0 and 3 mm/sec. The source is Co^{57} in Fe metal at 4.5°K, and the resonant absorber is a 1.7-mg/cm² Fe^{57} rolled foil at room temperature. Intensities correspond to total counting rates of gamma rays having energies between 10 and 18 kev.

temperatures of source and absorber of 6°K.[19] The central absorption peak of the rolled foil had a width at half height of 0.42 mm/sec and a depth 53% (uncorrected for background) below the intensity at high velocities. This width is approximately two times that expected for a thin absorber, and corresponds closely to the width expected for the thick foil used. The first strong satellite absorption lines at 2.23 mm/sec were well resolved, and had the theoretical ratio, 0.57, of depth compared to the central peak. Upon cooling the source to low temperatures, the central resonance peak broadened to 0.60 mm/sec. The shift is in close agreement with that observed previously for an absorber at room temperature and a source at the temperature of liquid air.[13] The increased resonance width can be attributed to differences between the hfs of the source and absorber, due to the variation of hfs with temperature; this effect has been studied in more detail at higher temperatures,[20,21] and will not be discussed here. The resonance pattern obtained with the rolled foil and with the source at 4.5°K is shown in Fig. 5. Vibration associated with the accelerations at the ends of the absorber travel became excessive at higher speeds; consequently, the first strong satellite lines were judged most suitable for examining the intensity asymmetry at low temperatures.

Preliminary experiments[5] conducted with the present source required the application of a large external magnetic field in the plane of the source foil. An appreciable remanent magnetization of the source could possibly lead to errors in the present work if, in addition, the absorber were magnetized. The latter condition could result from the method of preparation of the absorber. A combination of the two circumstances would change the relative intensities of the absorption dips at the several source-absorber speeds V, as a result of the net polarization of individual spectral components.[4] To a first-order approximation, a net polarization does not influence the relative contributions of individual lines, and hence, the temperature dependence of $R(V)$. Nevertheless, an experimental check of the net polarization of the spectra was made; the absorber orientation was rotated by 90 degrees about an axis normal to its plane. This rotation caused no perceptible changes in transmitted intensities, ensuring that the spectrum of Fig. 2 was appropriate to the experiment.

Experimental values of R (2.23 mm/sec) for temperatures between 4.5° and 0.85°K are shown in Fig. 6. Data points were taken over a period of several hours for each temperature, in order to accumulate the necessary number of counts, $\sim 10^7$, for adequate statistics. That the line does not pass through 1.00 at $1/T=0$ is probably due to a geometry effect. The counting rate with the absorber placed at the extremes of the normal travel was shown to be slightly different; as also noted earlier the absorber path length was slightly different for positive and negative velocities in this particular experiment. A systematic 0.3% change in the counting rate at one of the satellites used in obtaining the ratio would shift the ordinate in Fig. 6 by 0.015.

The experimental slope, $dR/dT^{-1}=0.0313\pm0.0021$ obtained by a least squares analysis is directly proportional to the magnitude of the field H at the Co^{57} nuclei. In order to deduce H, it is necessary to evaluate the coefficients in Eq. (18) for the actual foil thickness.

The total resonance cross section is given by the formula[17]

$$\sigma=2\pi\lambda^2\frac{2I_1+1}{2I_0+1}\left(\frac{1}{1+\alpha}\right)=1.48\times10^{-18}\ \text{cm}^2, \quad (21)$$

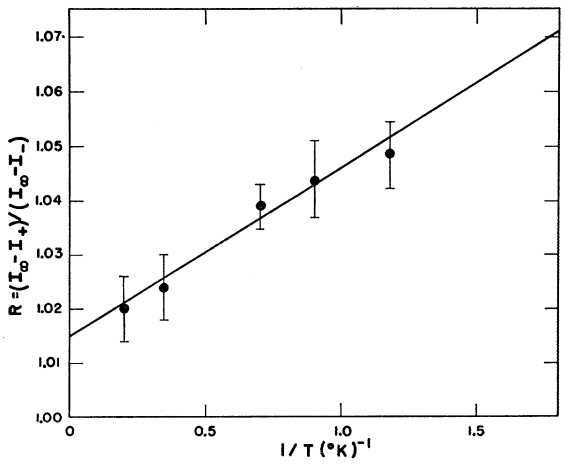

FIG. 6. Intensity ratio R for the 2.23-mm/sec resonant absorption dip at several temperatures between 4.5°K and 0.85°K.

[19] R. V. Pound and G. A. Rebka, Phys. Rev. Letters 4, 335 (1960).
[20] S. S. Hanna, Proceedings of the Allerton Park Conference on the Mössbauer Effect, University of Illinois, 1960 (unpublished), pp. 39–40; D. H. Vincent, R. S. Preston, J. Heberle, and S. S. Hanna, Bull. Am. Phys. Soc. 5, 428 (1960).
[21] D. E. Nagle, H. Frauenfelder, R. D. Taylor, D. R. F. Cochran, and B. T. Matthias, Phys. Rev. Letters 5, 364 (1960).

where λ is $(2\pi)^{-1}$ times the wavelength of the 14.4-kev radiation, I_1 and I_0 are the spins of the excited and ground states, respectively, and[22] $\alpha=15$ is the internal conversion coefficient. The calculated thickness parameter for the 1.73-mg/cm² foil is $x=27$. The effective thickness for the absorption lines having the intensity factors $w_{k'j'}=1/12$, 1/6, and 1/4 which overlap in the 2.23-mm/sec resonance are therefore $xw_{k'j'}/2=1.13$, 2.26, and 3.39, respectively. The temperature coefficients are calculated to be

$$\alpha_{M1}(V=2.23 \text{ mm/sec}, x=27)=2.19,$$
$$\alpha_{E2}(V=2.23 \text{ mm/sec}, x=27)=1.13.$$

The resulting formula for the ratio of intensities is, by Eq. (18),

$$R(V)=1+2.15\xi T^{-1}. \quad (22)$$

Comparison of Eq. (22) and the experimental value of $R(V)$ leads to the measured value of the Co^{57} level splitting,

$$\xi=(14.6\pm1.0)\times10^{-3}\text{°K}.$$

The hyperfine magnetic field H corresponding to this splitting is 300 ± 20 kilogauss.[12a]

V. DISCUSSION

The hfs magnetic field H acting on Co nuclei at low concentrations in Fe metal has been measured previously by other methods. Table I lists the values obtained to date. All measurements were made at low temperatures. The experimental uncertainties in all of the determinations are probably within a factor of 2 of the 7% estimated for the present work. There is no evident disagreement among the several measurements. Since the earlier studies could not be subject to the depolarization mechanisms discussed earlier in this paper, it is apparent that depolarization does not play an important role in the present technique. It is clear that we have observed no major depolarization such as occurs for Co^{57} in a Tutton salt.[11] We can conclude that the perturbing fields which are considered to be responsible for the Tutton salt results arise after the K-capture decay of the Co^{57}, and are probably due, in the Tutton salt, to long-lived holes in the outer electron shells. These holes are filled rapidly by the conduction electrons of the metal, in times that are short compared to the 10^{-8}-sec lifetime of the 136-kev state of Fe^{57}.

TABLE I. Hyperfine field H at Co nuclei in Fe metal.

Reference	Method	H (kilogauss)
Present work		300
(23)	Specific heat	320
(24)	Specific heat	315
(25)	Gamma-ray (Co^{60}) anisotropy	350

Finally, we note that the magnitude of H for Co in Fe metal is much closer to the field value of 333 kilogauss for Fe in Fe metal[4] than to the value 219 kilogauss for Co in Co metal.[15] It is not surprising that for these materials the effect of environment appears to dominate those interactions which may be ascribed to the individual atoms. Co differs from Fe in that it has one additional $3d$ electron, which is probably accepted into the unfilled $3d$ band of the Fe metal, thus leaving the Co nucleus in an environment characteristic of the surrounding Fe.

ACKNOWLEDGMENTS

We gratefully acknowledge the contributions of several people. L. Wilets of the University of Washington helped us to clarify our understanding of details of the decay scheme. R. Keil provided the thin rolled absorbers, and J. M. Dickinson assisted in the preparation of samples. W. E. Keller and D. R. F. Cochran, who collaborated on the initial experiments, encouraged and assisted us in the present work. R. R. Rylander constructed portions of the apparatus, and R. Hanft assisted in many of the measurements.

APPENDIX

Here we calculate the coefficients Q_{lj} which were introduced in Eq. (3). Q_{lj} is the probability that, if the Co^{57} nucleus initially has magnetic quantum number m_l, the decay will proceed to the Fe^{57} first excited state with magnetic quantum number m_j. It depends, in addition to the spins of the nuclear states involved, upon the character of the K capture, and on the multipolarity of the γ ray emitted in the transition between the second and first excited states.[26] As has been discussed in the text, the K capture is almost certainly Gamow-Teller allowed, and we will calculate the coefficients for both of the possible multipolarities, namely, $M1$ and $E2$. In case the radiation is not pure, but, as is realized for this γ ray, is a mixture of $M1$ and $E2$, there will in general be interference between the two components. However, the interference term vanishes when averaged over angle, so that if the source is unmagnetized it will have no effect, and the result obtained by adding the two contributions [see Eq. (18)] is correct.

If we denote the wave functions of Co^{57} and the second and first excited states of Fe^{57} by $\psi_{7/2}{}^{m_l}$, $\psi_{5/2}{}^{m'}$, and $\psi_{3/2}{}^{m_j}$, respectively, then the cobalt decay may be

[22] H. R. Lemmer, O. J. A. Segaert, and M. A. Grace, Proc. Phys. Soc. (London) **A68**, 701 (1955).
[23] V. Arp, D. Edmonds, and R. Petersen, Phys. Rev. Letters **3**, 212 (1959).
[24] N. Kurti, Suppl. J. Appl. Phys. **30**, 2155 (1960).
[25] A. V. Kogan, V. D. Kul'kov, L. P. Nikitin, N. M. Reinov, I. A. Sokolov, and M. F. Stel'makh, J. Exptl. Theoret. Phys. (U.S.S.R.) **39**, 47 (1960) [translation: Soviet Phys.—JETP **12**(**39**), 34 (1961)].
[26] It also depends on depolarizing forces, if any, which act in the intermediate state. We calculate it on the assumption that there are none.

TABLE II. Q_{lj} for $L=1$ ($M1$ γ ray).

m_l \ m_j	3/2	1/2	−1/2	−3/2
7/2	1	0	0	0
5/2	4/7	3/7	0	0
3/2	2/7	4/7	1/7	0
1/2	4/35	18/35	12/35	1/35
−1/2	1/35	12/35	18/35	4/35
−3/2	0	1/7	4/7	2/7
−5/2	0	0	3/7	4/7
−7/2	0	0	0	1

TABLE III. Q_{lj} for $L=2$ ($E2$ γ ray).

m_l \ m_j	3/2	1/2	−1/2	−3/2
7/2	3/7	4/7	0	0
5/2	24/49	9/49	16/49	0
3/2	22/49	4/49	19/49	4/49
1/2	12/35	38/245	72/245	51/245
−1/2	51/245	72/245	38/245	12/35
−3/2	4/49	19/49	4/49	22/49
−5/2	0	16/49	9/49	24/49
−7/2	0	0	4/7	3/7

represented by

$$\psi_{7/2}{}^{m_l} \rightarrow \sum_{m'} C(7/2, m_l|5/2, m'; 1, m_l-m') \times \psi_{5/2}{}^{m'} \chi_1{}^{m_l-m'}, \quad \text{(A1)}$$

where C is the usual Clebsch-Gordan coefficient and χ is a triplet S-wave function describing the emitted neutrino plus the absorbed electron. In turn, the decay of the second excited state is written

$$\psi_{5/2}{}^{m'} \rightarrow \sum_{m_j} C(5/2, m'|3/2, m_j; L, m'-m_j) \times \psi_{3/2}{}^{m_j} \gamma_L{}^{m'-m_j}, \quad \text{(A2)}$$

where γ_L represents the emitted γ ray of multipole order L. Upon substituting (A2) into (A1),

$$\psi_{7/2} \rightarrow \sum_{m_j} \sum_{m'} C(7/2, m_l|5/2m'; 1, m_l-m') \times C(5/2, m'|3/2, m_j; L, m'-m_j) \times \chi_1{}^{m_l-m'} \gamma_L{}^{m'-m_j} \psi_{3/2}{}^{m_j},$$

we find that the sum of squares of the contributions to the coefficient of $\psi_{3/2}{}^{m_j}$ is

$$Q_{lj}=\sum_{m'} |C(7/2, m_l|5/2, m'; 1, m_l-m') \times C(5/2, m'|3/2, m_j; L, m'-m_j)|^2.$$

The Clebsch-Gordan coefficients may be easily calculated, or found in tables, and the sum (which never contains more than 3 terms) evaluated numerically. The results are shown in Table II for $L=1$ (dipole γ ray), in Table III for $L=2$ (quadrupole γ ray).

Note added in proof. Recent examination of the hyperfine spectra of source and absorber by an unsplit absorber and source, respectively, has yielded relative intensities in the ratio 3:3.2:1, indicating that the samples were partially magnetized. Calculations based upon the revised spectrum increases the deduced value of the hyperfine field at Co^{57} nuclei to 375 kgauss. Further deviation of the actual intensity distribution from the distribution assumed in the text does not cause a further increase in the calculated field. Uncertainty in the intermediate magnetic history of the specimens prevents specifying the hyperfine field more precisely within the limits of 300 and 375 kgauss. Experiments now in progress should resolve the uncertainty in the near future.